

6-3-2015

Evolution of brown carbon in wildfire plumes

Haviland Forrister

Georgia Institute of Technology

Jiumeng Liu

Georgia Institute of Technology

Jack E. Dibb

University of New Hampshire, jack.dibb@unh.edu

Eric Scheuer

University of New Hampshire - Main Campus, Eric.Scheuer@unh.edu

Luke D. Ziemba

NASA

See next page for additional authors

Follow this and additional works at: https://scholars.unh.edu/earthsci_facpub



Part of the [Atmospheric Sciences Commons](#)

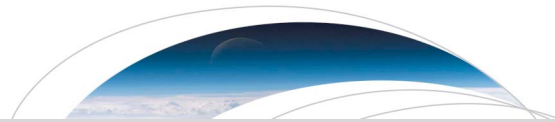
Recommended Citation

Forrister, H., et al. (2015), Evolution of brown carbon in wildfire plumes, *Geophys. Res. Lett.*, 42, 4623–4630, doi:10.1002/2015GL063897.

This Article is brought to you for free and open access by the Earth Sciences at University of New Hampshire Scholars' Repository. It has been accepted for inclusion in Earth Sciences Scholarship by an authorized administrator of University of New Hampshire Scholars' Repository. For more information, please contact nicole.hentz@unh.edu.

Authors

Haviland Forrister, Jiumeng Liu, Jack E. Dibb, Eric Scheuer, Luke D. Ziemba, Kenn L. Thornhill, Bruce Anderson, Glenn Diskin, Anne E. Perring, Joshua P. Schwarz, Pedro Campuzano-Jost, Douglas A. Day, Brett B. Palm, Jose L. Jimenez, Athanasios Nenes, and Rodney J. Weber



RESEARCH LETTER

10.1002/2015GL063897

Key Points:

- Biomass burning brown carbon has unknown lifecycle and atmospheric stability
- Brown carbon and aerosol properties from two fires are measured for 50 h
- Wildfire brown carbon lifetime was 9–15 h, but a small fraction is stable

Supporting Information:

- Figures S1–S4

Correspondence to:

R. J. Weber,
rodney.weber@eas.gatech.edu

Citation:

Forrister, H., et al. (2015), Evolution of brown carbon in wildfire plumes, *Geophys. Res. Lett.*, 42, 4623–4630, doi:10.1002/2015GL063897.

Received 17 MAR 2015

Accepted 11 MAY 2015

Accepted article online 14 MAY 2015

Published online 3 JUN 2015

Evolution of brown carbon in wildfire plumes

Haviland Forrister¹, Jiumeng Liu^{1,2}, Eric Scheuer³, Jack Dibb³, Luke Ziemba⁴, Kenneth L. Thornhill⁴, Bruce Anderson⁴, Glenn Diskin⁴, Anne E. Perring^{5,6}, Joshua P. Schwarz^{5,6}, Pedro Campuzano-Jost^{6,7}, Douglas A. Day^{6,7}, Brett B. Palm^{6,7}, Jose L. Jimenez^{6,7}, Athanasios Nenes^{1,8}, and Rodney J. Weber¹

¹School of Earth and Atmospheric Sciences, Georgia Institute of Technology, Atlanta, Georgia, USA, ²Now at Atmospheric Sciences and Global Change Division, Pacific Northwest National Laboratory, Richland, Washington, USA, ³Institute for the Study of Earth, Oceans, and Space, University of New Hampshire, Durham, New Hampshire, USA, ⁴NASA Langley Research Center, Hampton, Virginia, USA, ⁵Chemical Sciences Division, Earth System Research Laboratory, National Oceanic and Atmospheric Administration, Boulder, Colorado, USA, ⁶Cooperative Institute for Research in Environmental Sciences, University of Colorado Boulder, Boulder, Colorado, USA, ⁷Department of Chemistry and Biogeochemistry, University of Colorado Boulder, Boulder, Colorado, USA, ⁸School of Chemical and Biomolecular Engineering, Georgia Institute of Technology, Atlanta, Georgia, USA

Abstract Particulate brown carbon (BrC) in the atmosphere absorbs light at subvisible wavelengths and has poorly constrained but potentially large climate forcing impacts. BrC from biomass burning has virtually unknown lifecycle and atmospheric stability. Here, BrC emitted from intense wildfires was measured in plumes transported over 2 days from two main fires, during the 2013 NASA SEAC4RS mission. Concurrent measurements of organic aerosol (OA) and black carbon (BC) mass concentration, BC coating thickness, absorption Ångström exponent, and OA oxidation state reveal that the initial BrC emitted from the fires was largely unstable. Using back trajectories to estimate the transport time indicates that BrC aerosol light absorption decayed in the plumes with a half-life of 9 to 15 h, measured over day and night. Although most BrC was lost within a day, possibly through chemical loss and/or evaporation, the remaining persistent fraction likely determines the background BrC levels most relevant for climate forcing.

1. Introduction

Brown carbon (BrC) is the component of organic aerosol (OA) that absorbs light in the UV and visible spectral regions. Light absorption by BrC may globally offset the total climate cooling at the top of the atmosphere from direct radiative forcing of OA [Feng et al., 2013]. Vertical profiles of BrC measured in situ confirm its importance, as it can account for 20% of the aerosol direct radiative forcing at the top of the atmosphere [Liu et al., 2014]. Atmospheric BrC has two major sources: incomplete combustion of either fossil fuels [Bond, 2001; Yang et al., 2009; Zhang et al., 2011] or biomass [Hoffer et al., 2006; Chakrabarty et al., 2010; Hecobian et al., 2010; Kirchstetter and Thatcher, 2012; Desyaterik et al., 2013; Lack et al., 2013; Mohr et al., 2013] and secondary formation often involving carbonyl or aromatic compounds [Shapiro et al., 2009; Sareen et al., 2010; Kampf et al., 2012; Nguyen et al., 2012; Zarzana et al., 2012; Laskin et al., 2014; Nakayama et al., 2013; Yu et al., 2014]. Coupled charge transfer complexes formed in organic molecules may combine with individual chromophores and contribute to BrC absorption [Phillips and Smith, 2014]. When sensitive direct measurement techniques—such as light absorption of aerosol extracts—are used, BrC is found to be ubiquitous, present even in the remote continental troposphere at 10 km altitude [Kieber et al., 2006; Hecobian et al., 2010; Liu et al., 2014, 2015]. Recent studies suggest that aerosol components from biomass burning are more prevalent than previously thought [Hennigan et al., 2010, 2011; Bougiatioti et al., 2014] and may strongly contribute to this observed background BrC [Washenfelder et al., 2015].

As controls continue to reduce fossil fuel emissions and a changing climate potentially leads to more fires, both the relative and total impacts of biomass burning on air quality and climate forcing are expected to increase [Fuzzi et al., 2015]. Although studies have focused on the emissions of relatively briefly aged biomass burning BrC for use in large-scale modeling by predicting BrC behavior and radiative forcing effects from a ratio of black carbon (BC) to OA [Saleh et al., 2014], there is a growing body of evidence that atmospheric BrC evolves differently from both BC and bulk OA, owing to production of BrC from secondary organic aerosol and loss of BrC from photobleaching [Lee et al., 2014; Zhong and Jang, 2014; Zhao et al., 2015], volatilization, or aerosol-phase reactions. In order to understand the difference between

BrC and bulk OA evolution and ultimately determine the effects of BrC on climate, a focused effort to measure its atmospheric distribution and evolution is needed.

In this study, we determine the evolution of BrC related to large wildfire plumes sampled from near emission to over 2 days of atmospheric transport. To our knowledge, this study constitutes the first reported evolution of brown carbon from biomass burning smoke in the natural atmosphere.

2. Method

In situ measurements were conducted on board the NASA DC-8 airborne platform as part of the SEAC4RS (Studies of Emissions, Atmospheric Composition, Clouds and Climate Coupling by Regional Surveys) mission. Sampling occurred from 6 August to 23 September 2013 over the western, central, and southeastern regions of the continental U.S. SEAC4RS followed the Deep Convective Clouds and Chemistry campaign, where the DC-8 flew with the same instrument payload. The instrumentation used to measure BrC and identify biomass burning plumes is described in detail by *Liu et al.* [2014] and is briefly summarized here.

BrC was determined by direct measurement of the light absorption spectra over a wide wavelength range from liquid extracts of aerosol collected on Teflon (EMD Millipore) filters. Individual filters each collected aerosol mass (for particles less than 4.1 μm aerodynamic diameter) for 5 to 10 min and were stored at nominally -10°C . A 2.5 m path length liquid waveguide capillary cell, a UV-visible light source (200 to 800 nm range), and a spectrophotometer provided a measure of BrC with higher sensitivity than established aerosol optical methods. Filters were extracted first in water, then methanol, to extract most biomass burning BrC components [*Chen and Bond, 2010*]. Light absorption spectra relative to that of the pure solvent were determined for each sample. Here, we focus on BrC light absorption of the dissolved aerosol in the solvent averaged between 360 and 370 nm (in Mm^{-1}) and refer to it simply as BrC (see *Hecobian et al.* [2010] for method). Complete spectra are also provided.

Aerosol light absorption coefficients ($b_{\text{ap}}(\lambda)$) at three wavelengths (470, 532, and 660 nm) were measured with a particle soot absorption photometer (PSAP) for aerosols below 4.1 μm aerodynamic diameter and were corrected for artifacts associated with filter-based optical absorption measurements as described by *Virkkula* [2010]. Absorption Ångström exponents were determined from the 470 and 532 nm wavelength pair by

$$\text{AAE}_{\text{PSAP}} = - \frac{\ln(b_{\text{ap,PSAP}}(532)) - \ln(b_{\text{ap,PSAP}}(470))}{\ln(532) - \ln(470)} \quad (1)$$

Particle chemical composition was determined with a high-resolution time of flight aerosol mass spectrometer (HR-ToF-AMS) [*DeCarlo et al., 2006*] that measured bulk aerosol particles nominally below 1 μm aerodynamic diameter. Here, we use the overall OA concentrations and the O/C (oxygenation) [*Aiken et al., 2008*]. O/C was determined using the organic mass fraction of the HR-ToF-AMS data using the updated calibrations of *Canagaratna et al.* [2015]. The mass ratio of biomass burning tracer signal (arising from levoglucosan and related molecules) to OA, f_{60} , was calculated from the HR-ToF-AMS data by taking the ratio of the signal at m/z 60 to the total organic mass signal [*Cubison et al., 2011*]. Refractory black carbon (rBC) mass concentrations were determined with a SP2 (single-particle soot photometer) and were corrected for particle sizes outside the measurement range [*Schwarz et al., 2008*]. SP2 data were also used to estimate rBC coating thickness for dried aerosol sampled in the individual plumes using the methodology of *Schwarz et al.* [2008] for particles with 3 to 5 fg rBC mass content. The dry modal coating thickness was reported every 5 to 10 min. Carbon monoxide (CO) was measured as a mixing ratio using diode laser spectrometry to make a differential absorption CO measurement at 1 s intervals [*Sachse et al., 1987*].

In the analysis, BrC was first plotted against the CO concentration to identify which filter sampling periods corresponded to the most intense regions of the plume and to exclude filters with a significant sample integration period not associated with the plume. For each aircraft transit through a plume, BrC data from the filters were selected based on filter sample integration times corresponding to the most significant CO enhancements within the plume (CO "peaks"). If more than one filter sample existed within a given peak, the data were averaged over those filter sampling times. Once the in-plume filters were identified, all parameters of interest were merged to the filter sampling times if the data covered were greater than 75%

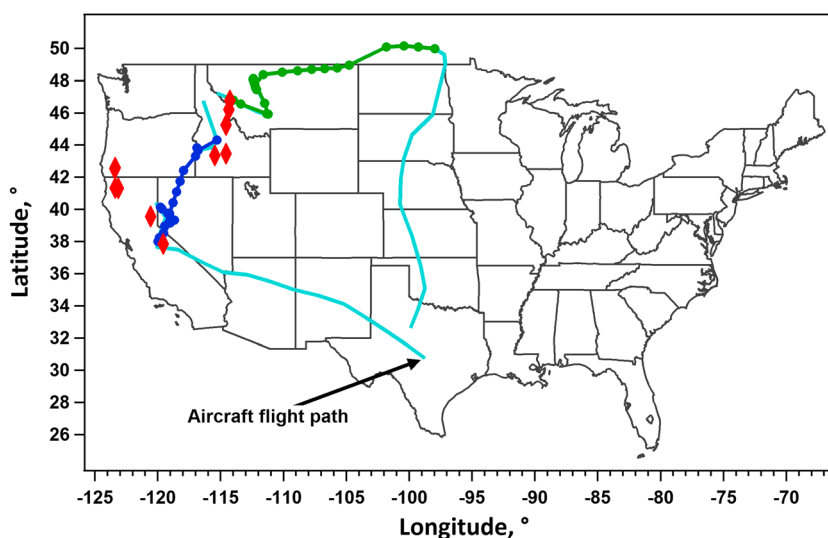


Figure 1. Map of the SEAC4RS flight trajectory, with Rim fire 1 biomass burning data points (blue), Rim fire 2 biomass burning data points (green), and regional wildfires identified (red).

of the filter integration time; these merged data were retrieved from the NASA SEAC4RS archive (the 19 May 2014 merge), except for the HR-ToF-AMS data that were updated on 24 October 2014. Aerosol data are reported at STP (1 atm, 273.15 K).

To account for dilution with plume transport, normalized excess mixing ratios (NEMRs) [Hobbs *et al.*, 2003] were calculated using CO as the conservative tracer (e.g., $\Delta X/\Delta CO$). Background concentrations for the various NEMRs and CO were determined from data averaged before and after each plume intercept. NEMRs were generated for BrC, rBC, and OA. Intensive parameters, including the AAE, rBC coating thickness, O/C, and f60, are not presented as NEMRs.

Air mass transport times, in hours since emission, are used as the metric for degree of plume evolution based on Hybrid Single-Particle Lagrangian Integrated Trajectory (HYSPPLIT) back trajectories from the point of aircraft measurement to the fire source location. The fire source latitude and longitude were retrieved from INCIWEB reports (<http://inciweb.nwccg.gov/>) for the Rim and Elk Complex Fires described below. For each plume measurement, the amount of time the air mass was exposed to sunlight during transport from the fire to the point of measurement was also estimated in order to investigate possible photochemical effects on BrC evolution. HYSPPLIT back trajectories verified that the various plume intercepts analyzed were from a common fire or region of fires given the limited degree of spatial resolution available by this method.

3. Results

3.1. The Rim Fires

Although many plumes from both agricultural and wildfires were intercepted during SEAC4RS, here we focus on the Rim fires (named due to their proximity to the scenic point “Rim of the World”) since these were the largest plumes detected and hence most amenable to aerosol analyses via filters. The Rim fires produced smoke plumes studied over two consecutive days. On the first day, 26 August 2013, the aircraft investigated the smoke downwind from an extensive fire near Yosemite National Park, CA, referred to as the Rim 1 fire. Throughout this flight, the smoke was tracked as it moved northeast through Nevada, Oregon, and Idaho, where other regional fires were by and large avoided by the aircraft (Figure 1). On the following day, 27 August 2013, the goal was to pick up this plume and continue to track it. However, the Rim 1 plume passed over another active burning region in Idaho, the Elk Creek Complex fire, and then moved from Idaho, through Montana, and into Manitoba, Canada (Figure 1). The plume from this second day is referred to as Rim 2, since delineating the smoke from the Yosemite and Elk Creek Complex fires is not clear-cut. In the following, we analyze the BrC evolution in two ways: (1) assuming all smoke is from the Yosemite fire and (2) assuming that the primary smoke sampled during the Rim 2 flight was from the

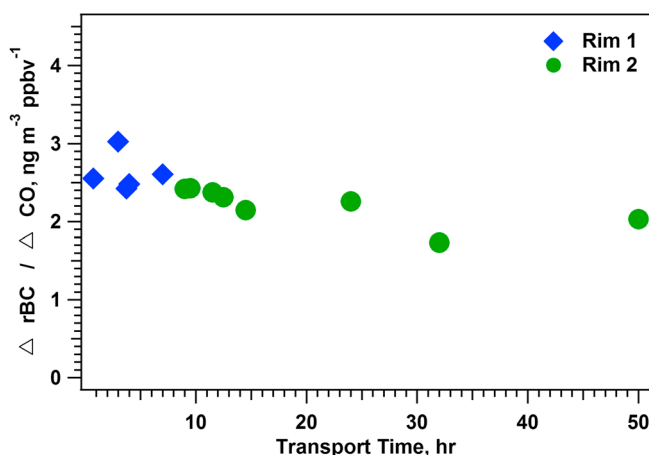


Figure 2. Evolution of refractory black carbon (rBC) in the Rim smoke plumes. Transport time for Rim 2 is calculated assuming smoke was from the Elk Creek Complex fire.

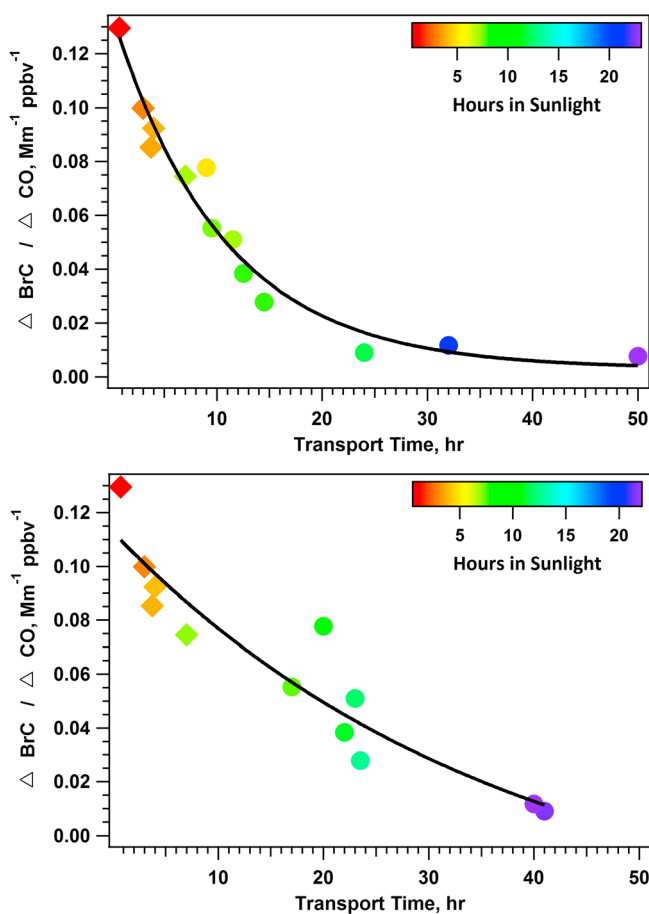


Figure 3. Evolution of BrC in the Rim smoke plumes. Diamond symbol indicates Rim 1; circle symbol indicates Rim 2. Color designates amount of time the smoke was exposed to sunlight during transport. The line is an exponential fit indicating the loss of BrC. Transport times are calculated for Rim 2 using (top) the Elk Creek Complex fire as the source and (bottom) the Yosemite fire as the source.

Elk Creek Complex fire. This provides a discrete range in the evolution times of BrC. Other parameters of interest are plotted assuming the Rim 2 smoke is solely from the Elk Creek Complex fire, for simplicity. The Rim 1 data track from about 1 to 7 h of plume age, while the Rim 2 data track from 9 to 50 h if assuming the source is the Elk Creek Complex fire (or 17 to 40 h, assuming the Yosemite fire). The combined Rim 1 and Rim 2 data provide an opportunity to study the evolution of BrC and other aerosol properties for over 2 days of transport, corresponding to a transport distance of 1500 km.

3.2. Measurements in Smoke Plume

For the two Rim flights, the plumes are easily identified close to the fires by high correlations between BrC and CO concentrations (for both flights combined, BrC and CO were correlated with $r^2 = 0.98$), indicating BrC enhancements are associated with smoke plumes (see supporting information Figure S1 for BrC and CO time series).

To test our analysis method, given uncertainty imposed by the filter sampling times and plume widths, we first plot the NEMR for rBC for all smoke plumes sampled (Figure 2), assuming Rim 2 data resulted from the Elk Creek Complex fire. CO and rBC are both emitted from biomass burning and should both be approximately conserved in transport in the free troposphere in the absence of precipitation over these timescales. Thus, little change is expected with plume age, as is seen. At the beginning of both the Rim 1 and Rim 2 fires, there was scatter in the $\Delta rBC / \Delta CO$ (supporting information Figure S2), which appears to result from smoke plumes from separate local fires having different rBC relative to CO emissions. These data are excluded from the overall plume evolution for the following analysis.

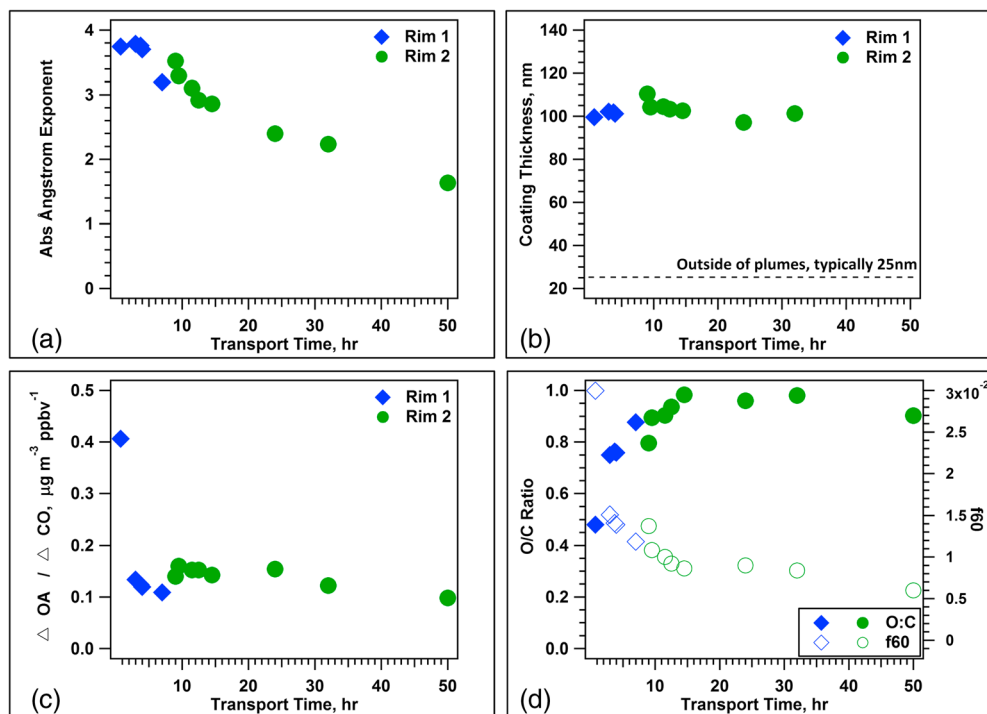


Figure 4. Evolution of other pertinent aerosol properties in the Rim smoke plumes, including (a) the absorption Ångström exponent, (b) rBC coating thickness, (c) $\Delta OA/\Delta CO$, and (d) OA oxygen-to-carbon ratio and f_{60} (tracer of biomass burning primary OA). Transport time for Rim 2 is calculated using the Elk Creek Complex fire as the smoke source.

Figure 3 shows the evolution of BrC concentration (via proxy solution extract light absorption at 365 nm), where the transport time was calculated assuming Rim 2 originated from both the Elk Creek Complex and the Yosemite fires. In contrast to $\Delta rBC/\Delta CO$, which was relatively constant over time, BrC in these plumes decreased over transport with an approximate half-life of 9 h, assuming the Elk Creek Complex fire, or 15 h, assuming the Yosemite fire as the source of Rim 2 smoke. If any mixing of the smoke from the two fires occurred, the half-life should fall between these two extremes. The color scale in Figure 3 represents the approximate amount of sunlight that the sampled smoke aerosol was exposed to, with specified values in hours provided in supporting information Figure S3. With increased sunlight exposure, the BrC continued to decrease. However, after about 12 h, continued sunlight exposure showed no effect; it is likely that all the chromophores that could be affected by photochemistry or photobleaching were eliminated by this time. This result is consistent with laboratory experiments showing BrC photobleaching [Zhong and Jang, 2014; Lee et al., 2014; Zhao et al., 2015], although the photobleaching experiments found much shorter half-lives of a few minutes to a few hours and/or do not correlate with the solar cycle. Reduced light absorption with time suggests a BrC loss mechanism such as chemical bleaching (chemical reactions resulting in the destruction of the chromophores). Evaporation (or volatilization) may also be occurring. BrC absorption at all wavelengths measured follows a similar decrease (supporting information Figure S4), indicating net light absorption should also decrease over time.

As expected if BrC is being bleached or removed, the net aerosol AAE should decrease with age, as can be seen in Figure 4a, where AAEs of 3.5 to 4.0 near the fire drop toward 1 at long ages, the approximate AAE for pure BC. The AAEs reach about 1.5 after 50 h of transport, roughly the value recorded in this study of background conditions. This decrease in AAE highly correlates with the decrease in BrC, with $r^2 = 0.83$ (Figure 5a). The rBC is highly coated in the plumes, with a coating thickness typically near 100 nm, significantly thicker than outside the plumes where it averages 25 nm. However, the coating thickness does not vary with plume age (Figure 4b), indicating that the OA coating the rBC particles must be nonvolatile. Application of shell-and-core Mie theory has suggested that rBC light absorption is enhanced with decreasing wavelength in a manner similar to BrC [Bond et al., 2006; Lack and Cappia, 2010], so coatings might alter the light absorption spectral properties of rBC. However, since both rBC and the coatings atop

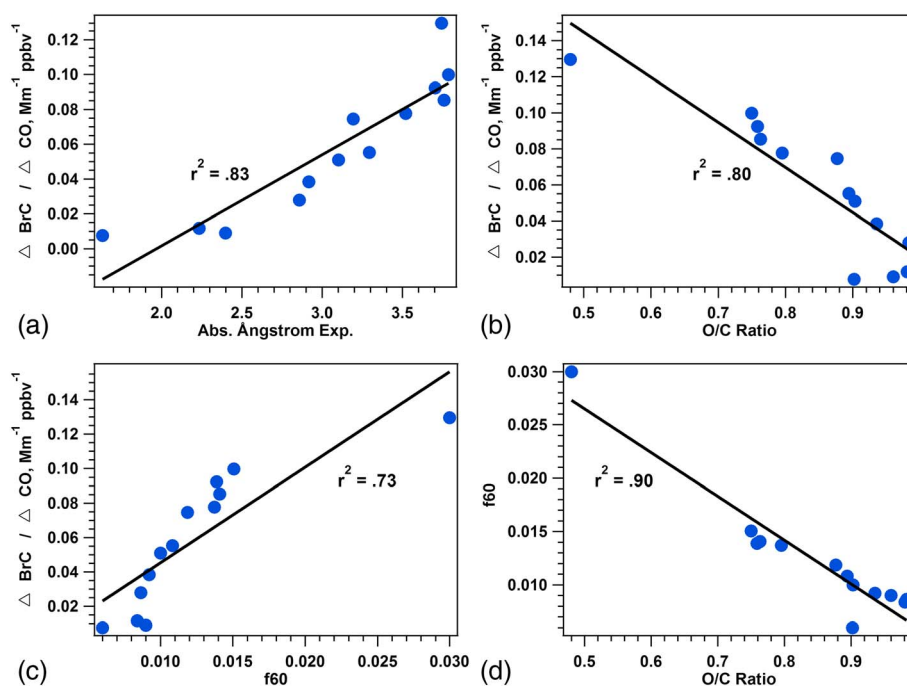


Figure 5. Correlations between (a) $\Delta \text{BrC} / \Delta \text{CO}$ and the absorption Ångström exponent, (b) $\Delta \text{BrC} / \Delta \text{CO}$ and O/C, (c) $\Delta \text{BrC} / \Delta \text{CO}$ and f_{60} , and (d) f_{60} and O/C.

rBC were observed to be constant, the decrease in AAE with age must be due to the loss of some other light-absorbing compound—specifically BrC—and cannot be explained by a shrinking shell over a rBC core.

Since the chromophore-containing molecules that comprise BrC are expected to constitute a small mass fraction of bulk OA, differing trends in $\Delta \text{OA} / \Delta \text{CO}$ and $\Delta \text{BrC} / \Delta \text{CO}$ are not surprising (Figure 4c). OA initially decreases rapidly with a half-life of less than 2 h, followed by little change after about 3 h. In these plumes, evaporation losses apparently dominated over any secondary organic aerosol formation processes. Having a steady thickness of rBC coating while bulk OA decreases is not inconsistent since the coating mass concentration is small relative to OA (estimated to be <10%, assuming OA and BC densities of 0.9 and 0.75 g cm^{-3} , respectively). In addition, OA is produced mainly by smoldering combustion, while rBC is mainly by flaming combustion; thus, the small fraction of OA associated with rBC particles may have different composition from the bulk of OA coming from different processes in the fire. As the plume ages, the O/C (oxygenation) of the OA increases and f_{60} (biomass burning OA relative to OA) decreases (Figure 4d), which has been previously observed [Cubison *et al.*, 2011]. The decay in f_{60} is likely due to a combination of evaporation and oxidation, as studied before [Molina *et al.*, 2004; Robinson *et al.*, 2007; Lambe *et al.*, 2012; Donahue *et al.*, 2014], and indicates that although the bulk OA concentration stabilizes, its molecular composition changes with time. This is consistent with the evolving BrC. Indeed, the rate of change of both O/C and f_{60} better follow the decrease in BrC rather than the decrease of OA. The chemical transformations of the observed biomass burning OA, including changes in BrC, seem to occur approximately simultaneously, as indicated by correlations between the various variables (see Figure 5). Overall, this correlation between increasing O/C and decreasing BrC and f_{60} suggests a possible linked process, like photooxidation [Zhao *et al.*, 2015]. A photooxidation process leading to BrC loss is also consistent with the greater sunlight exposures correlating with decreases in BrC (Figure 3). Other processes could also be occurring, such as loss of volatile BrC. Further experiments and analyses of more ambient smoke plumes are needed to provide a better understanding of the life cycle of BrC from biomass burning.

4. Conclusions

The scale of the Rim 1 and Rim 2 fires allowed for an unprecedented investigation into the evolution of wildfire smoke in the ambient atmosphere. These data show that absorption at 365 nm (Figure 3), and over

the complete wavelength range associated with BrC (supporting information Figure S4), decreased with a half-life of roughly 9 to 15 h. While the processes causing loss of BrC in the Rim smoke plumes combine to remove most emitted BrC within a day, this decay rate is typically far slower than losses observed solely due to photobleaching in current environmental chamber experiments with realistic conditions. However, both ambient and chamber data [Lee *et al.*, 2014; Zhao *et al.*, 2015; Zhong and Jang, 2014] imply that predictions of the prevalence or optical impacts of BrC cannot simply be inferred from emission or near-emission measurements without considering complex processing with age. Our data are unique in that plume evolution was observed over a sufficient time that a stable fraction of BrC was observed to persist. Approximately 6% of the BrC emitted remained above background levels even after 50 h following emission and was no longer affected by sunlight. This BrC should be further investigated as it likely accounts for the ubiquitous BrC previously observed throughout the troposphere in our previous study with this aircraft payload, which was shown to have important radiative impacts [Liu *et al.*, 2014]. Since the total and relative impact of biomass burning on air quality is expected to increase [Fuzzi *et al.*, 2015], future studies should focus on the mechanisms responsible for the reduction of light absorption following biomass burning we observed and the difference in timescales with current laboratory experiments. Knowledge of the mechanisms governing biomass burning BrC behavior in the atmosphere would allow us to determine the overall climate forcing due to biomass burning BrC and the degree to which it will affect air quality, in general, in the future.

Acknowledgments

All data used in this paper were collected as part of the NASA SEAC4RS mission and became available to the general public on 15 October 2014 through the NASA data archive. This project was funded by GIT NASA contracts NNX12AB83G and NNX14AP74G and UNH NASA contract NNX12AB80G. P.C.J., D.A.D., and J.L.J. were supported by NASA NNX12AC03G.

The Editor thanks two anonymous reviewers for their assistance in evaluating this paper.

References

- Aiken, A. C., P. DeCarlo, J. H. Kroll, D. R. Worsnop, J. A. Huffman, K. S. Docherty, I. M. Ulbrich, C. Mohr, J. R. Kimmel, and D. Sueper (2008), O/C and OM/OC ratios of primary, secondary, and ambient organic aerosols with high-resolution time-of-flight aerosol mass spectrometry, *Environ. Sci. Technol.*, *42*, 4478–85, doi:10.1021/es703009q.
- Bond, T. C. (2001), Spectral dependence of visible light absorption by carbonaceous particles emitted from coal combustion, *Geophys. Res. Lett.*, *28*, 4075–4078, doi:10.1029/2001GL013652.
- Bond, T. C., G. Habib, and R. W. Bergstrom (2006), Limitations in the enhancement of visible light absorption due to mixing state, *J. Geophys. Res.*, *111*, D20211, doi:10.1029/2006JD007315.
- Bougiatioti, A., et al. (2014), Processing of biomass burning aerosol in the eastern Mediterranean during summertime, *Atmos. Chem. Phys.*, *14*, 4793–4807, doi:10.5194/acp-14-4793-2014.
- Canagaratna, M. R., et al. (2015), Elemental ratio measurements of organic compounds using aerosol mass spectrometry: Characterization, improved calibration, and implications, *Atmos. Chem. Phys.*, *15*, 253–272, doi:10.5194/acp-15-253-2015.
- Chakrabarty, R. K., H. Moosmuller, L.-W. A. Chen, K. Lewis, W. P. Arnott, C. Massoleni, M. K. Dubey, C. E. Wold, W. M. Hao, and S. M. Kreidenweis (2010), Brown carbon in tar balls from smoldering biomass combustion, *Atmos. Chem. Phys.*, *10*, 6363–6370, doi:10.5194/acp-10-6363-2010.
- Chen, Y., and T. C. Bond (2010), Light absorption by organic carbon from wood combustion, *Atmos. Chem. Phys.*, *10*, 1773–1787, doi:10.5194/acp-10-1773-2010.
- Cubison, M. J., et al. (2011), Effects of aging on organic aerosol from open biomass burning smoke in aircraft and laboratory studies, *Atmos. Chem. Phys.*, *11*, 12,049–12,064, doi:10.5194/acp-11-12049-2011.
- DeCarlo, P. F., et al. (2006), Field-deployable, high-resolution, time-of-flight aerosol mass spectrometer, *Anal. Chem.*, *78*, 8281–8289, doi:10.1021/ac061249n.
- Desyaterik, Y., Y. Sun, X. Shen, T. Lee, X. Wang, T. Wang, and J. L. Collett (2013), Speciation of brown carbon in cloud water impacted by agricultural biomass burning in eastern China, *J. Geophys. Res. Atmos.*, *118*, 7389–7399, doi:10.1002/jgrd.50561.
- Donahue, N., A. Robinson, E. Trumpf, I. Riipinen, and J. Kroll (2014), Volatility and aging of atmospheric organic aerosol, *Top. Curr. Chem.*, *339*, 97–143.
- Feng, Y., V. Ramanathan, and V. R. Kotamarthi (2013), Brown carbon: A significant atmospheric absorber of solar radiation?, *Atmos. Chem. Phys.*, *13*, 8607–8621, doi:10.5194/acp-13-8607-2013.
- Fuzzi, S., et al. (2015), Particulate matter, air quality and climate: Lessons learned and future needs, *Atmos. Chem. Phys. Discuss.*, *15*, 521–744, doi:10.5194/acpd-15-521-2015.
- Hecobian, A., X. Zhang, M. Zheng, N. Frank, E. S. Edgerton, and R. J. Weber (2010), Water-soluble organic aerosol material and the light-absorption characteristics of aqueous extracts measured over the southeastern United States, *Atmos. Chem. Phys.*, *10*, 5965–5977, doi:10.5194/acp-10-5965-2010.
- Hennigan, C. J., A. P. Sullivan, J. L. Collett, and A. L. Robinson (2010), Levoglucosan stability in biomass burning particles exposed to hydroxyl radicals, *Geophys. Res. Lett.*, *37*, L09806, doi:10.1029/2010GL043088.
- Hennigan, C. J., et al. (2011), Chemical and physical transformations of organic aerosol from the photo-oxidation of open biomass burning emissions in an environmental chamber, *Atmos. Chem. Phys.*, *11*, 11,995–12,037, doi:10.5194/acp-11-7669-2011.
- Hobbs, P. V., P. Sinha, R. J. Yokelson, T. J. Christian, D. R. Blake, S. Gao, T. W. Kirchstetter, T. Novakov, and P. Pilewskie (2003), Evolution of gases and particles from a savanna fire in South Africa, *J. Geophys. Res.*, *108*(D13), 8485, doi:10.1029/2002JD002352.
- Hoffer, A., A. Gelencser, P. Guyon, G. Kiss, O. Schmid, G. P. Frank, P. Artaxo, and M. O. Andreae (2006), Optical properties of humic-like substances (HULIS) in biomass-burning aerosols, *Atmos. Chem. Phys.*, *6*, 3563–3570, doi:10.5194/acp-6-3563-2006.
- Kampf, C. J., R. Jakob, and T. Hoffmann (2012), Identification and characterization of aging products in the glyoxal/ammonium sulfate system—Implications for light-absorbing material in atmospheric aerosols, *Atmos. Chem. Phys.*, *12*, 6323–6333, doi:10.5194/acp-12-6323-2012.
- Kieber, R. J., R. F. Whitehead, S. N. Reid, J. D. Willey, and P. J. Seaton (2006), Chromophoric dissolved organic matter (CDOM) in rainwater, southeastern North Carolina, USA, *J. Atmos. Chem.*, *54*, 21–41.
- Kirchstetter, T. W., and T. L. Thatcher (2012), Contribution of organic carbon to wood smoke particulate matter absorption of solar radiation, *Atmos. Chem. Phys. Discuss.*, *12*, 5803–5816, doi:10.5194/acp-12-6067-2012.

- Lack, D. A., and C. D. Cappa (2010), Impact of brown and clear carbon on light absorption enhancement, single scatter albedo and absorption wavelength dependence of black carbon, *Atmos. Chem. Phys.*, *10*, 4207–4220, doi:10.5194/acp-10-4207-2010.
- Lack, D. A., R. Bahreini, J. M. Langridge, J. B. Gilman, and A. M. Middlebrook (2013), Brown carbon absorption linked to organic mass tracers in biomass burning particles, *Atmos. Chem. Phys.*, *13*, 2415–2422, doi:10.5194/acp-13-2415-2013.
- Lambe, A. T., et al. (2012), Transitions from functionalization to fragmentation reactions of laboratory secondary organic aerosol (SOA) generated from the OH oxidation of alkane precursors, *Environ. Sci. Technol.*, *46*, 5430–5437, doi:10.1021/es300274t.
- Laskin, J., A. Laskin, S. A. Nizkorodov, P. Roach, P. Eckert, M. K. Gilles, B. Wang, H. J. Lee, and Q. Hu (2014), Molecular selectivity of brown carbon chromophores, *Environ. Sci. Technol.*, *48*(20), 12,047–12,055, doi:10.1021/es503432r.
- Lee, H. J., P. K. Aiona, A. Laskin, J. Laskin, and S. A. Nizkorodov (2014), Effect of solar radiation on the optical properties and molecular composition of laboratory proxies of atmospheric brown carbon, *Environ. Sci. Technol.*, *48*, 10,217–10,226, doi:10.1021/es502515r.
- Liu, J., et al. (2014), Brown carbon in the continental troposphere, *Geophys. Res. Lett.*, *41*, 2191–2195, doi:10.1002/2013GL058976.
- Liu, J., et al. (2015), Brown carbon aerosol in the North American continental troposphere: Sources, abundance, and radiative forcing, *Atmos. Chem. Phys. Discuss.*, *15*, 5959–6007.
- Mohr, C., et al. (2013), Contribution of nitrated phenols to wood burning brown carbon light absorption in Detling, United Kingdom during winter time, *Environ. Sci. Technol.*, *47*, 6316–6324, doi:10.1021/es400683v.
- Molina, M. J., A. V. Ivanov, S. Trakhtenberg, and L. T. Molina (2004), Atmospheric evolution of organic aerosol, *Geophys. Res. Lett.*, *31*, L22104, doi:10.1029/2004GL020910.
- Nakayama, T., K. Sato, Y. Matsumi, T. Imamura, A. Yamazaki, and A. Uchiyama (2013), Wavelength and NO_x dependent complex refractive index of SOAs generated from the photooxidation of toluene, *Atmos. Chem. Phys.*, *13*, 531–545, doi:10.5194/acp-13-531-2013.
- Nguyen, T. B., P. B. Lee, K. M. Updyke, D. L. Bones, J. Laskin, A. Laskin, and S. A. Nizkorodov (2012), Formation of nitrogen- and sulfur-containing light-absorbing compounds accelerated by evaporation of water from secondary organic aerosols, *J. Geophys. Res.*, *117*, D01207, doi:10.1029/2011JD016944.
- Phillips, S. M., and G. D. Smith (2014), Further evidence for charge transfer complexes in brown carbon aerosols from excitation–emission matrix fluorescence spectroscopy, *Environ. Sci. Technol. Lett.*, *1*, 382, doi:10.1021/jp510709e.
- Robinson, A. L., N. M. Donahue, M. K. Shrivastava, E. A. Weitkamp, A. M. Sage, A. P. Grieshop, T. E. Lane, J. R. Pierce, and S. N. Pandis (2007), Rethinking organic aerosols: Semivolatile emissions and photochemical aging, *Science*, *315*, 1259–1262, doi:10.1126/science.1133061.
- Sachse, G. W., G. F. Hill, L. O. Wade, and M. G. Perry (1987), Fast-response, high-precision carbon monoxide sensor using a tunable diode laser absorption technique, *J. Geophys. Res.*, *92*, 2071–2081, doi:10.1029/JD092iD02p02071.
- Saleh, R., et al. (2014), Brownness of organics in aerosols from biomass burning linked to their black carbon content, *Nat. Geosci.*, *7*, 647–650, doi:10.1038/NGEO2220.
- Sareen, N., A. N. Schwieter, E. L. Shapiro, D. Mitroo, and V. F. McNeil (2010), Secondary organic material formed by methylglyoxal in aqueous aerosol mimics, *Atmos. Chem. Phys.*, *10*, 997–1016, doi:10.5194/acp-10-997-2010.
- Schwarz, J. P., et al. (2008), Coatings and their enhancement of black carbon light absorption in the tropical atmosphere, *J. Geophys. Res.*, *113*, D03203, doi:10.1029/2007JD009042.
- Shapiro, E. L., J. Szprengiel, N. Sareen, C. N. Jen, M. R. Giordano, and V. F. McNeill (2009), Light-absorbing secondary organic material formed by glyoxal in aqueous aerosol mimics, *Atmos. Chem. Phys.*, *9*, 2289–2300, doi:10.5194/acp-9-2289-2009.
- Virkkula, A. (2010), Correction of the calibration of the 3-wavelength Particle Soot Absorption Photometer (3λPSAP), *Aerosol Sci. Technol.*, *44*(8), 706–712, doi:10.1080/02786826.2010.482110.
- Washenfelder, R. A., et al. (2015), Biomass burning dominates brown carbon absorption in the rural southeastern United States, *Geophys. Res. Lett.*, *42*, 653–664, doi:10.1002/2014GL062444.
- Yang, M., S. G. Howell, J. Zhuang, and B. J. Huebert (2009), Attribution of aerosol light absorption to black carbon, brown carbon, and dust in China—Interpretations of atmospheric measurements during EAST-AIRE, *Atmos. Chem. Phys.*, *9*, 2035–2050, doi:10.5194/acp-9-2035-2009.
- Yu, L., J. Smith, A. Laskin, C. Anastasio, J. Laskin, and Q. Zhang (2014), Chemical characterization of SOA formed from aqueous-phase reactions of phenols with the triplet excited state of carbonyl and hydroxyl radical, *Atmos. Chem. Phys.*, *14*, 13,801–13,816, doi:10.5194/acp-14-13801-2014.
- Zarzana, K. J., D. O. D. Haan, M. A. Freedman, C. A. Hasenkopf, and M. A. Tolbert (2012), Optical properties of the products of α -dicarbonyl and amine reactions in simulated cloud droplets, *Environ. Sci. Technol.*, *46*(9), 4845–4851, doi:10.1021/es2040152.
- Zhang, X., Y.-H. Lin, J. D. Surratt, P. Zotter, A. S. H. Prevot, and R. J. Weber (2011), Light-absorbing soluble organic aerosol in Los Angeles and Atlanta: A contrast in secondary organic aerosol, *Geophys. Res. Lett.*, *38*, L21810, doi:10.1029/2011GL049385.
- Zhao, R., A. K. Y. Lee, L. Huang, X. Li, F. Yang, and J. P. D. Abbatt (2015), Photochemical processing of aqueous atmospheric brown carbon, *Atmos. Chem. Phys. Discuss.*, doi:10.5194/acpd-15-2957-2015.
- Zhong, M., and M. Jang (2014), Dynamic light absorption of biomass burning organic carbon photochemically aged under natural sunlight, *Atmos. Chem. Phys.*, *14*, 1517–1525, doi:10.5194/acp-14-1517-2014.